# Supporting Information

## Synergistic electrical and light management enables efficient monolithic inorganic perovskite/organic tandem solar cells with over 24% efficiency

Shan Jiang,[a,b] Ruyue Wang,[a] Minghua Li,[a,*] Runnan Yu,[a] Fuzhi Wang,[b] and Zhan'ao Tan [a,*]

[a] Beijing Advanced Innovation Center for Soft Matter Science and Engineering, College of Chemical Engineering, College of Materials Science and Engineering, Beijing University of Chemical Technology, Beijing 100029, China

[b] State Key Laboratory of Alternate Electrical Power System with Renewable Energy Sources, North China Electric Power University, Beijing 102206, China

Corresponding author. Email: limh2022@buct.edu.cn; tanzhanao@mail.buct.edu.cn

S. Jiang and R. Wang contributed equally.

**Experimental Section**

**Materials:** Lead bromide ($PbBr_2$, 99.9%), lead iodide ($PbI_2$, 99.9%), cesium iodide (CsI, 99.9%), were purchased from Xi'an Polymer Light Technology Corp. PM6, BTP-eC9, PFN-Br were purchased from Solarmer. Molybdenum Trioxide ($MoO_3$) was purchased from Acros, tin dioxide ($SnO_2$) (15% water), 1-chloronaphthalene, DIO, dimethyl sulfoxide (DMSO, anhydrous, ≥99.8%), chlorobenzene (≥99.9%), chloroform (≥99.9%) were purchased from Alfa Aesea. Cl@MZO synthesized according to references.

**Precursor preparation:** $SnO_2$ precursor solution was prepared by diluted Tin (IV) oxide (15% in $H_2O$ colloidal dispersion) 3 times with ultra-pure water was stirred overnight at room temperature. 1.2M $CsPbI_2Br$ perovskite precursor solution was prepared by dissolving CsI (312 mg), $PbI_2$ (277 mg), $PbBr_2$ (220 mg) in 1 mL DMSO. Dissolve 10 mg of PM6 in 1mL CB solution and prepare an HTL solution with a concentration of 10 mg/mL stir at 5 hours at room temperature. Dissolve PM6: BTP-eC9 in CF at a D/A weight ratio of 1:1.2, 1:1.8, and 1:2.4, with 18, 22, and 25 mg $ml^{-1}$ total concentrations, respectively. Heat and stir at 50 ℃ for 3 hours to obtain PM6: BTP-eC9 solutions with the different donor-to-acceptor ratios. In addition, add CN with a volume ratio of 0.5% to each solution before spin coating. Dissolve 0.5 mg PFN-Br in 1 mL methanol solution and stir overnight at room temperature to prepare ETL solution.

**Device Fabrication:** For the PSCs, ETL solution was spin-coated on pre-cleaned ITO and annealed at 150 ℃ for 30 mins. Then, the obtained ITO/$SnO_2$ or Cl@MZO was put in an $N_2$-filled glovebox. $CsPbI_2Br$ precursor was spin-coated on the ETL film at 1000 rpm 5 s and 2500 rpm 30s. The film was annealed at 42 ℃ for 2 min and 250 ℃ for 10 mins to form $CsPbI_2Br$ film. PM6 (10 mg/mL), dissolved in chlorobenzene was deposited on $CsPbI_2Br$ film at 3000 rpm for 30s to form HTL. Finally, the 10 nm $MoO_3$ layer and 100 nm Ag electrode were thermal-evaporated onto $CsPbI_2Br$ film.

For the single junction OSCs, PFN-Br precursor was spin-coated on pre-cleaned ITO in an $N_2$-filled glovebox. The PM6: BTP-eC9 solution was spin-coated on PFN-Br film at 3000 rpm 30 s to obtain organic photoactive film. Finally, the 10 nm $MoO_3$

layer and 100 nm Ag electrode were thermal-evaporated onto photoactive film.

For the TSCs, after depositing the HTL of the front cell, the 8 nm $MoO_3$ layer and 1-2 nm Ag electrode were sequentially thermal-evaporated onto the HTL layer. Then, PFN-Br (0.5 mg/mL, dissolved in methanol) was spin-coated at 4000 rpm for 30 s on the electrode. Next, the deposition conditions of the rear cells' organic photoactive layer are consistent with that of single junction OSCs. Finally, the 10 nm $MoO_3$ layer and 100 nm Ag electrode were thermal-evaporated to obtain complete TSCs.

**Instrumentation and characterization:** The current-voltage (*J-V*) curves were measured under the illumination of AM1.5G (100 mW $cm^{-2}$) by a Keithley 2400 digital source meter. EQE spectrum was obtained by Zolix SCS10-X150-DSSC system. For TSCs, the EQE test is performed using a filtered bias light shone onto the sample surface. When testing the EQE of front PSCs, the light with wavelengths below 700 nm in the bias light is filtered out. When testing the EQE of rear OSCs, light with wavelengths higher than 550 nm in the bias light is filtered out. The active area of devices is 4 $mm^2$. UV-vis absorption and transmittance spectra were tested by Shimadzu UV-3600. PL and TRPL measurements were detected by Edinburgh Fluorescence Spectrometer (FLS 980). SEM images were measured using a Zeiss Sigma 300 Field Emission Electron Microscopy at acceleration voltages of 3 kV. AFM measurements were performed using SPM-9700HTTM. TA spectroscopy was tested by a regenerative amplified Ti: sapphire laser system (Coherent) as the laser source and an EOS spectrometer (Ultrafast Systems LLC) as the spectrometer. XRD was tested using PANalytical Empyrean. FTIR was recorded by BRUKER 1295-6214 and the films for FITR measurements were deposited on the KBr substrate. Test the $n_k$ value of the device using an ellipsometer (Horiba Uvisel FUV) for square distribution simulation.

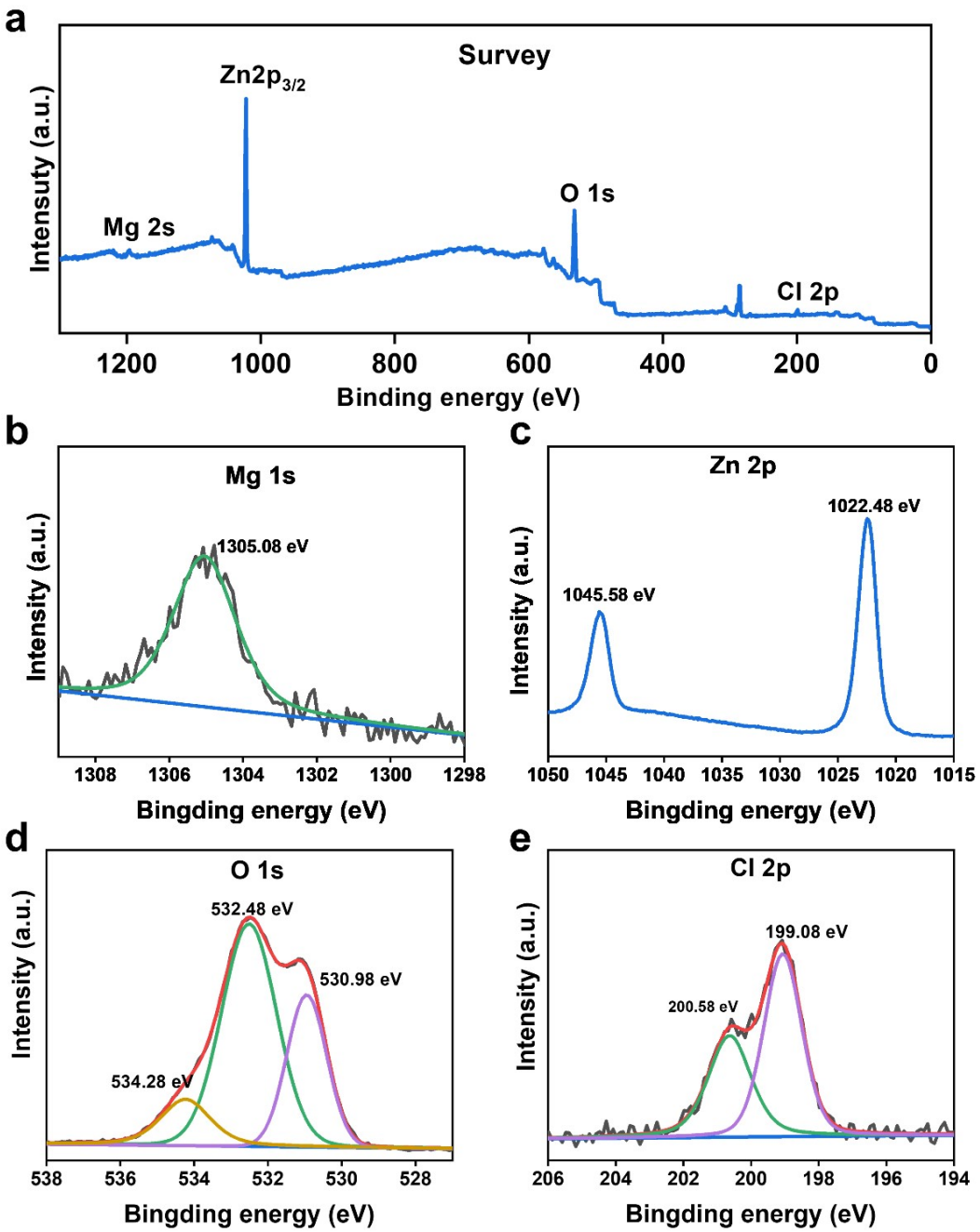


**Figure S1.** High-resolution XPS signals of (a) XPS survey spectra of Cl@MZO, (b) Mg 1s, (c) Zn 2p (d) O 1s and (e) Cl 2p for Cl@MZO films.

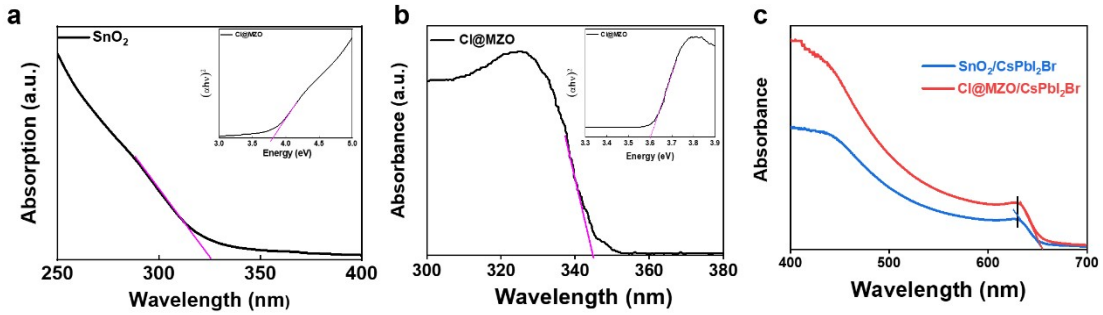


**Figure S2.** UV-vis absorption spectra of (a) $SnO_2$, (b) Cl@MZO, and (c) $CsPbI_2Br$ film.

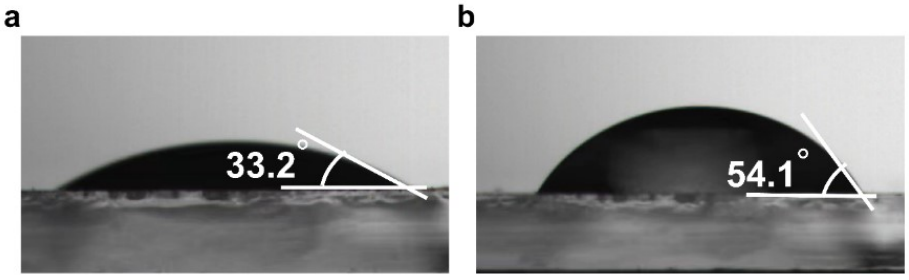


**Figure S3.** The water contact angle of (a) $SnO_2$/$CsPbI_2Br$ and (b) Cl@MZO/$CsPbI_2Br$ films.

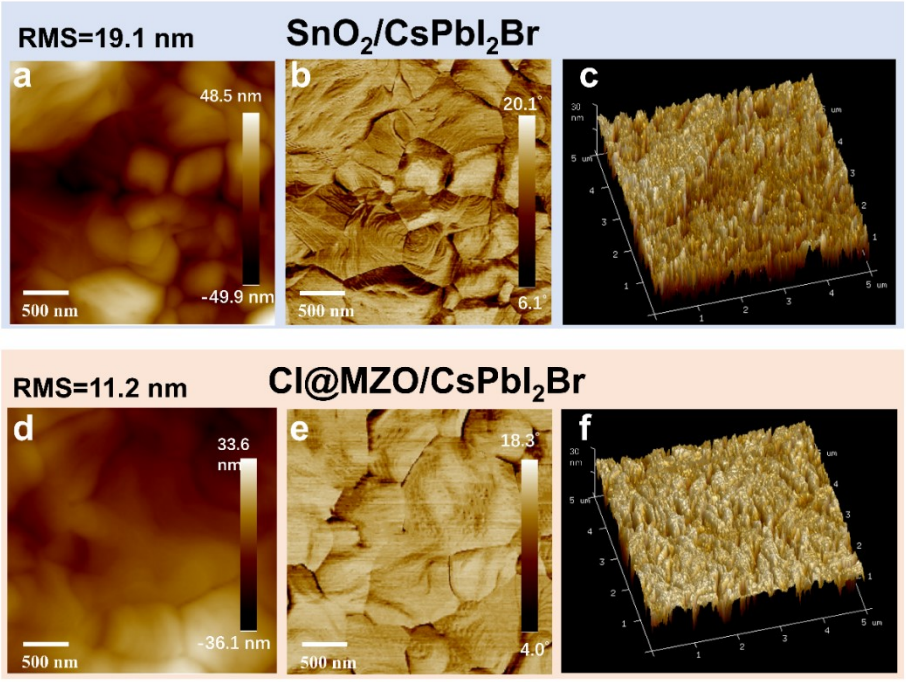


**Figure S4.** (a) AFM height image, (b) phase image and (c) 3D AFM image of $SnO_2$/$CsPbI_2Br$ film. (d) AFM height image, (e) phase image and (f) 3D AFM image

of Cl@MZO/$CsPbI_2Br$ film.

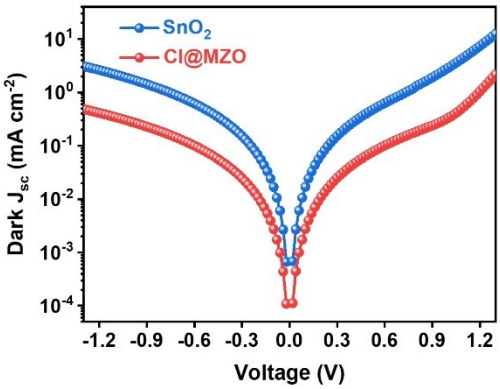


**Figure S5.** Dark *J–V* characteristics of single junction $CsPbI_2Br$ devices.

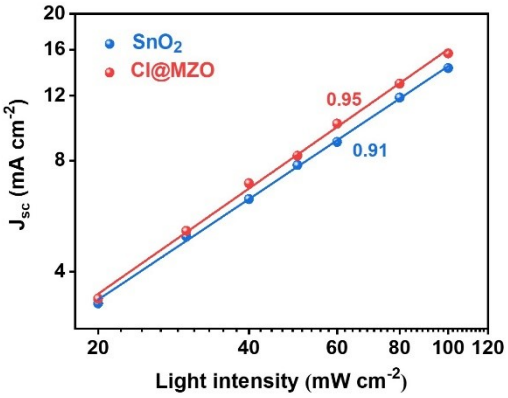


**Figure S6.** $J_{sc}$ as a function of $P_{light}$ for single junction $CsPbI_2Br$ devices.

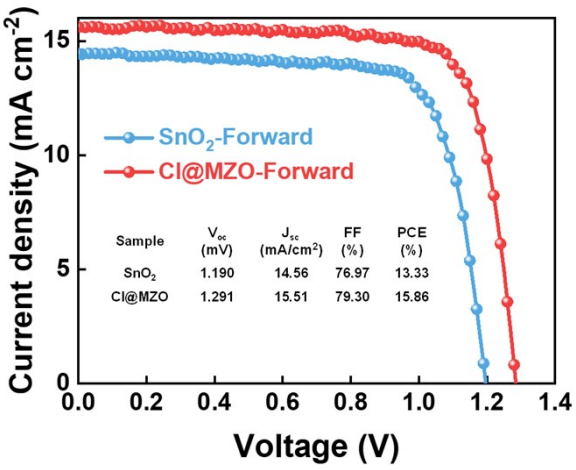


**Figure S7.** *J–V* curves of $CsPbI_2Br$ PSCs measured at forward scan.

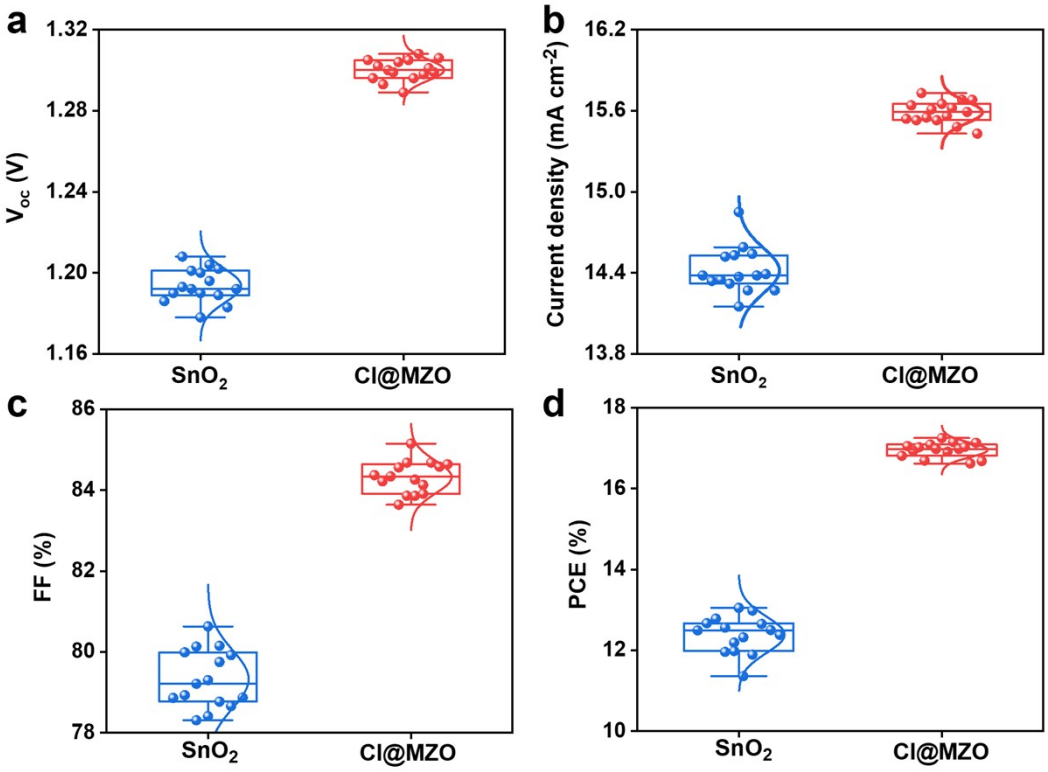


**Figure S8.** The box-line statistics of (a) $V_{oc}$, (b) $J_{sc}$, (c)FF and (d)PCE for the $CsPbI_2Br$ devices.

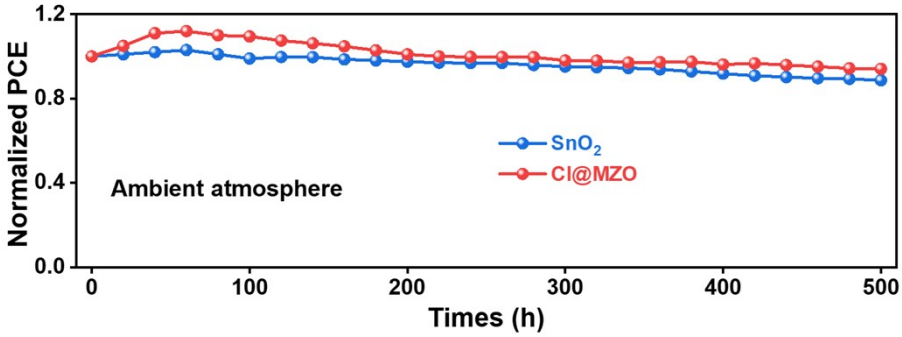


**Figure S9.** Air stability of $CsPbI_2Br$ single-junction devices based on $SnO_2$ and Cl@MZO ETLs.

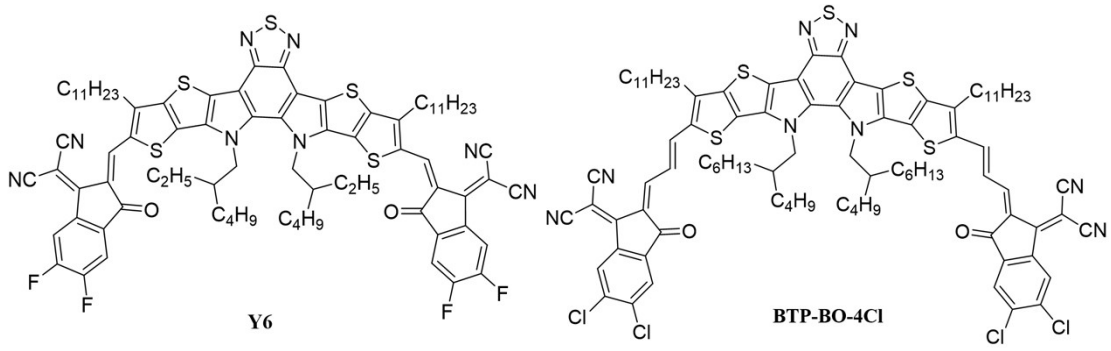


**Figure S10.** Chemical structure of Y6 and BTP-BO-4Cl.

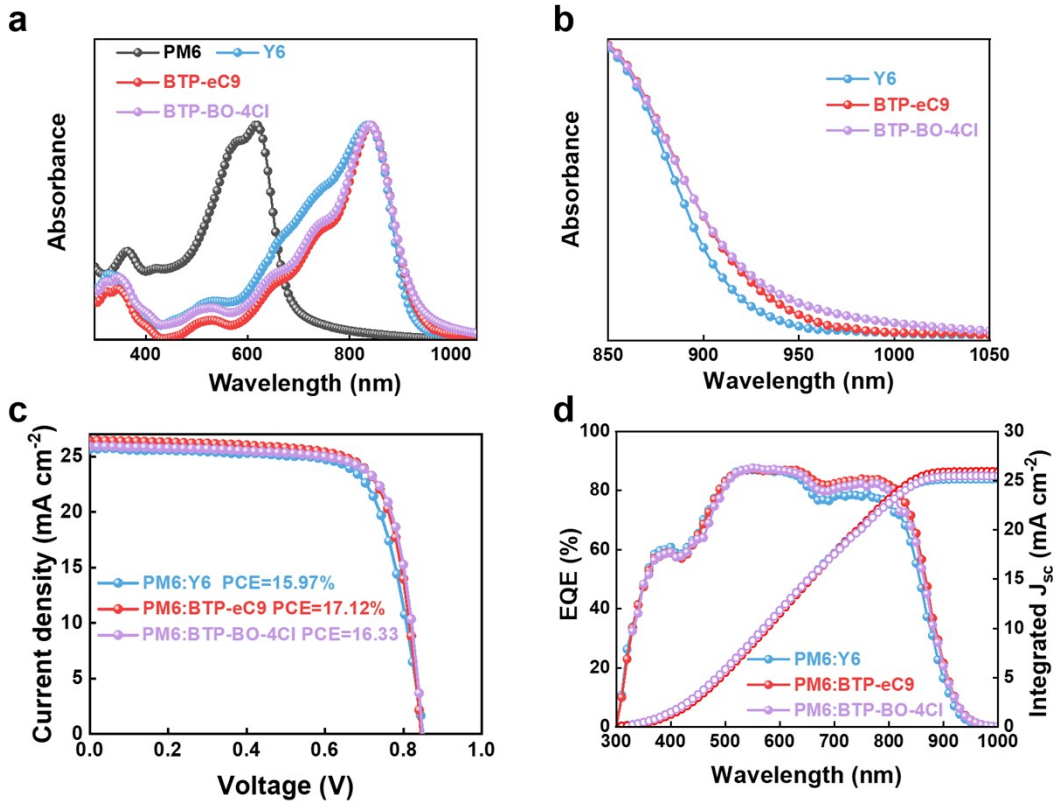


**Figure S11.** (a) The UV-vis spectra of PM6, Y6, BTP-eC9 and BTP-BO-4Cl films. (b) The comparison of UV-visible absorption spectra in NIR region of Y6, BTP-eC9 and BTP-BO-4Cl films. (c) *J*−*V* and (d) EQE curves of devices based on different active layers.

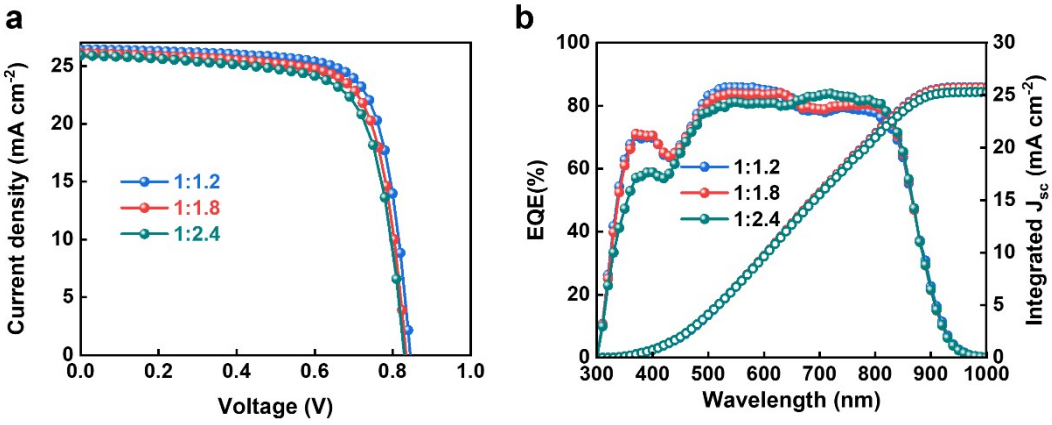


**Figure S12.** (a) $J-V$ and (b) EQE curve of devices based on different ratios of donor and acceptor.

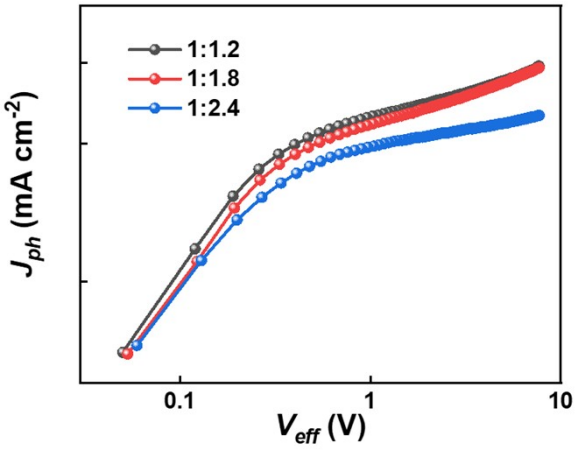


**Figure S13.** The $J_{ph}-V_{eff}$ curve of OSCs based on PM6: BTP-eC9 blend films with different D/A ratios.

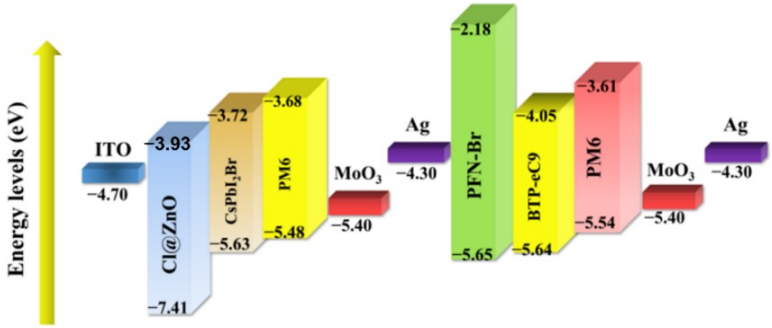


**Figure S14.** Schematic energy level diagram of TSCs.

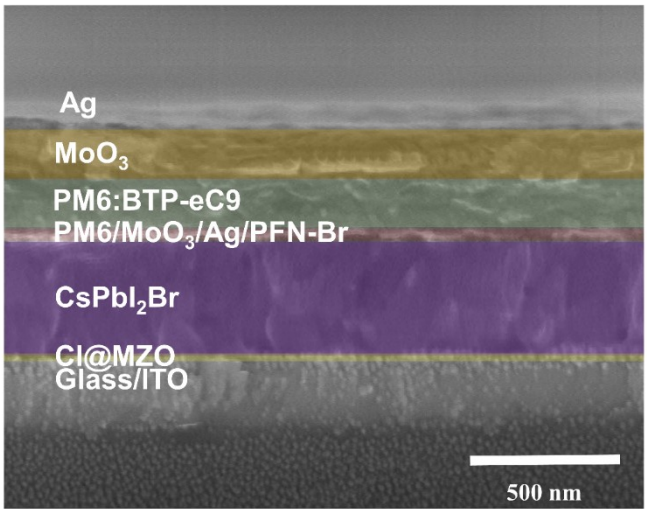


**Figure S15.** Cross-sectional SEM image of complete TSCs.

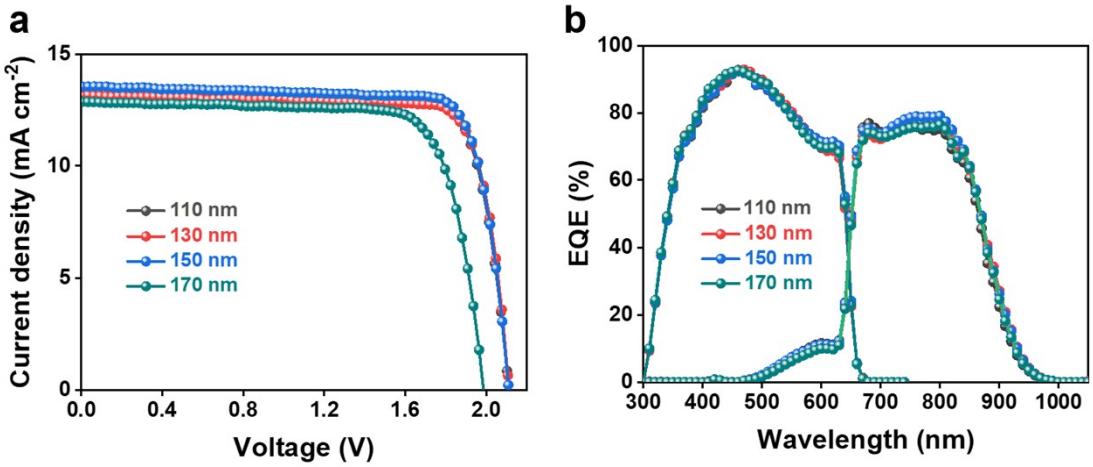


**Figure S16.** (a) *J*−*V* and (b) EQE curves of tandem devices using PM6: BTP-eC9 blend films.

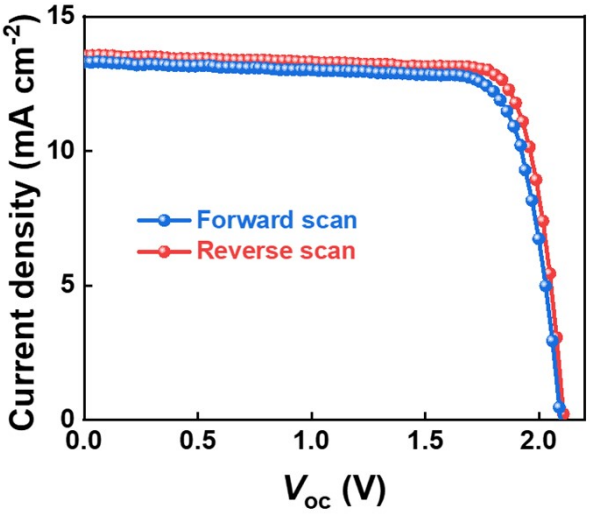


**Figure S17.** *J*–*V* curves of TSC measured at different scan directions.

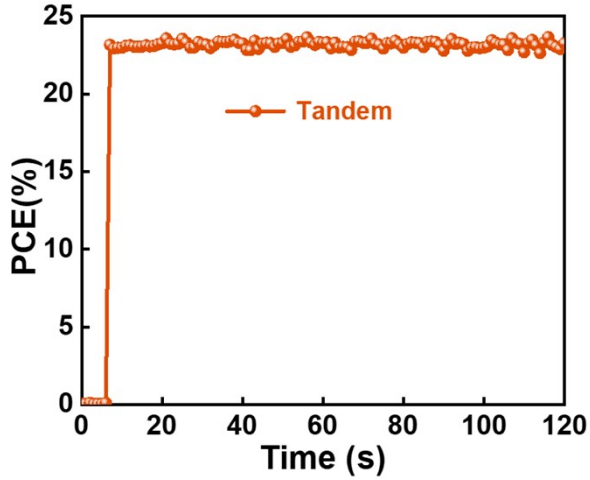


**Figure S18.** Stabilized efficiency output of maximum power point tracking.

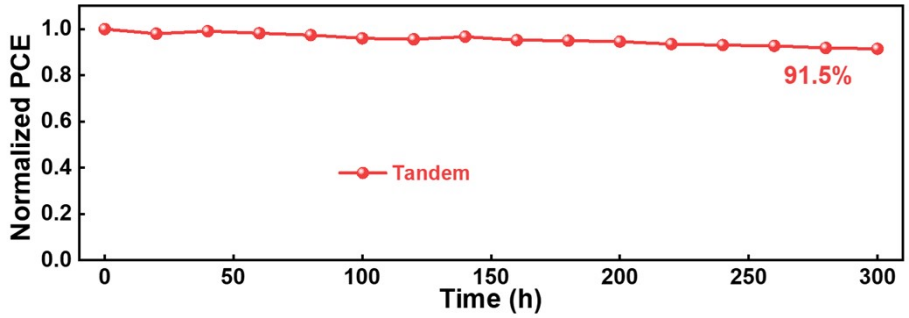


**Figure S19.** Photostability of TSC in $N_2$ without encapsulation.

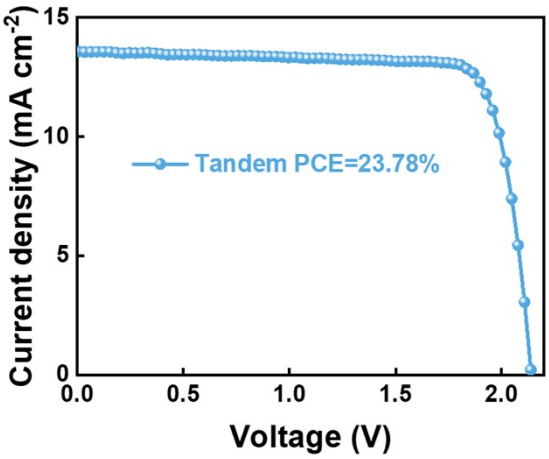


**Figure S20.** Initial efficiency of stability testing devices.

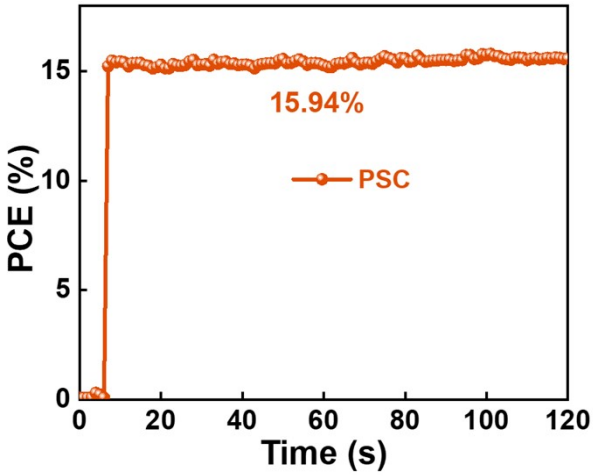


**Figure S21.** Stabilized power output of maximum power point tracking for single junction PSCs.

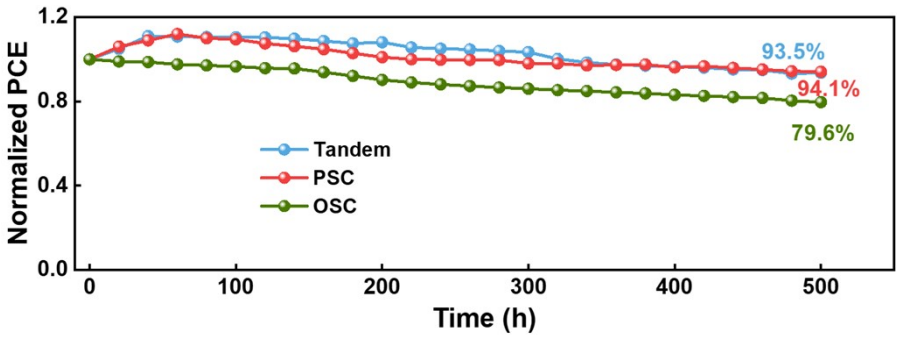


**Figure S22.** Air stability of the front PSC, rear OSC and tandem devices.

**Table S1.** Photovoltaic parameters of single-junction cells based on various fabrication conditions under different illuminations.

| D/A ratio | $V_{oc}$ (V) | $J_{sc}$ (mA cm$^{-2}$) | FF (%) | PCE (%) | $J_{EQE}$ (mA cm$^{-2}$) |
|---|---|---|---|---|---|
| 1:1.2 | 0.840 | 26.43 | 77.11 | 17.12 | 25.91 |
| 1:1.8 | 0.833 | 26.32 | 73.65 | 16.15 | 25.82 |
| 1:2.4 | 0.829 | 25.95 | 71.67 | 15.41 | 25.32 |
| 1:1.2 (Filtered) | 0.830 | 12.89 | 77.12 | 18.94 | 12.50 |
| 1:1.8 (Filtered) | 0.833 | 13.24 | 75.65 | 19.17 | 12.92 |
| 1:2.4 (Filtered) | 0.834 | 13.29 | 71.67 | 18.25 | 13.01 |

**Table S2.** Parameters of the $CsPbI_2Br$/PM6: BTP-eC9-based tandem device based on blend films with different thicknesses.

| Thicknesses (nm) | $V_{oc}$ (V) | $J_{sc}$ (mA cm$^{-2}$) | FF (%) | PCE (%) | $J_{EQE}$ (mA cm$^{-2}$) |
|---|---|---|---|---|---|
| 110 | 2.109 | 13.02 | 81.36 | 22.35 | 13.25/12.75 |
| 130 | 2.110 | 13.17 | 81.29 | 22.58 | 13.25/12.98 |
| 150-R | 2.111 | 13.55 | 81.68 | 23.35 | 13.21/13.20 |
| 150-F | 2.085 | 13.32 | 80.24 | 22.28 | |
| 170 | 2.069 | 12.87 | 77.53 | 20.65 | 13.15/12.68 |

**Table S3.** Parameters of TSC based on different ratios of donor and acceptor

| D/A ratio | $V_{oc}$ (V) | $J_{sc}$ (mA cm$^{-2}$) | FF (%) | PCE (%) | $J_{EQE}$ (mA cm$^{-2}$) |
|---|---|---|---|---|---|
| 1:1.2 | 2.141 | 12.99 | 81.02 | 22.52 | 13.19/12.53 |
| 1:1.8 | 2.139 | 13.36 | 81.28 | 23.22 | 13.25/12.75 |
| 1:2.4 | 2.121 | 12.92 | 79.10 | 21.67 | 13.10/12.62 |

**Table S4.** Photovoltaic parameters of PSC, OSCs and TSCs.

| | $V_{oc}$ (V) | $J_{sc}$ (mA cm$^{-2}$) | FF (%) | PCE (%) | $J_{EQE}$ (mA cm$^{-2}$) |
|---|---|---|---|---|---|
| Front PSC | 1.305 | 15.54 | 83.98 | 17.05 | 15.07 |
| Rear OSCs (1:1.8) | 0.833 | 26.32 | 73.65 | 16.15 | 25.82 |
| TSCs | 2.152 | 13.89 | 80.57 | 24.07 | 13.49/13.47 |

**Table S5.** Summary of state-of-the-art monolithic inorganic perovskite/organic TSCs.

| Device structure | $V_{oc}$ (V) | $J_{sc}$ (mA cm$^{-2}$) | FF (%) | PCE (%) | Ref |
|---|---|---|---|---|---|
| ITO/$TiO_2$/IC60BA: PSEHTT/PEDOT: PSS/$TiO_2$/Graphene/$MAPbI_3$/Spiro-OMeTAD/Au | 1.86 | 8.73 | 72.0 | 11.28 | [1] |
| ITO/$SnO_2$/$CsPbI_2Br$/PTAA/$MoO_3$/Au/ZnO/PTB7-Th: COi8DFIC: PC71BM/$MoO_3$/Ag | 1.71 | 11.98 | 73.4 | 15.04 | [2] |
| ITO/ZnO/$SnO_2$/$CsPbI_2Br$/PDCBT/$MoO_3$/Ag/ZnO/PM6: BTP-eC9/$MoO_3$/Ag | 1.95 | 12.46 | 75.59 | 18.38 | [3] |
| ITO/ZnO/$CsPbI_2Br$/P3HT/MoOx/Au/ZnO/PTB7-Th: IEICO-4F/MoOx/Ag | 1.73 | 12.94 | 80.1 | 18.04 | [4] |
| ITO/$SnO_2$/$CsPbI_{2.1}Br_{0.9}$/PMACl/PBDB-T/$MoO_3$/Ag/ZnO NP/PM6: BTP-eC9/$MoO_3$/Ag | 1.89 | 12.77 | 74.81 | 18.06 | [5] |
| ITO/$SnO_2$/$CsPbI_2Br$/P3HT/$MoO_3$/Ag/PFN-Br/PTB7-Th: IEICO-4F/$MoO_3$/Ag | 1.82 | 13.15 | 71.68 | 17.24 | [6] |
| ITO/ZnO/$CsPbI_2Br$/Poly-TPD/$MoO_3$/Ag/PFN-Br/PM6:Y6-BO/$MoO_3$/Ag | 1.96 | 13.30 | 80.3 | 21.10 | [7] |
| ITO/$SnO_2$/$CsPbI_{1.8}Br_{1.2}$/TACl/PBDB-T/$MoO_3$/Au/PFN-Br/ZnO/PM6:Y6/$MoO_3$/Al | 2.05 | 13.36 | 76.82 | 21.04 | [8] |
| ITO/$SnO_2$/ZnO/$CsPbI_2Br$/PTAA/$MoO_3$/Au/ZnO NPs/D18:Y6/$MoO_3$/Ag | 2.05 | 13.07 | 75.3 | 20.18 | [9] |
| ITO/ZnO/$SnO_2$/$CsPbI_2Br$/$MoO_3$/Ag/PFN-Br/PM6:Y6 /$MoO_3$/Ag | 2.097 | 13.09 | 75.2 | 20.6 | [10] |
| ITO/$SnO_2$/$CsPbI_{1.9}Br_{1.1}$/PM6/$MoO_3$/Au/ZnO/PFN/D18-Cl: N3: $PC_{61}BM$/$MoO_3$/Ag | 2.15 | 13.43 | 80.25 | 23.17 | [11] |

| | | | | | |
|---|---|---|---|---|---|
| ITO/ZnO/$SnO_2$/MAFm/$CsPbI_2Br$/MAFm/PDCBT/$MoO_3$/Au//ZnO/BCP/PM6:CH1007/$MoO_3$/Ag | 2.10 | 14.23 | 77.79 | 23.21 | [12] |
| ITO/ZnO/$CsPbI_2Br$/PM6/$MoO_3$/Ag/PFN-Br/PM6: BTP-eC9/$MoO_3$/Ag | 2.152 | 13.89 | 80.57 | 24.07 | **This work** |

## References


1. A. R. Bin, M. Yusoff and J. Jang, *Chem. Commun.*, 2016, **52**, 5824-5827.
2. Q. Zeng, L. Liu, Z. Xiao, F. Liu, Y. Hua, Y. Yuan and L. Ding, *Sci. Bull.*, 2019, **64**, 885-887.
3. S. K. Xie, R. X. Xia, Z. Chen, J. J. Tian, L. Yan, M. R. Ren, Z. C. Li, G. C. Zhang, Q. F. Xue, H. L. Yip and Y. Cao, *Nano Energy*, 2020, **78**, 105238.
4. H. Aqoma, I. F. Imran, F. T. A. Wibowo, N. V. Krishna, W. Lee, A. K. Sarker, D. Ryu and S. Y. Jang, *Adv. Energy. Mater.*, 2020, **10**, 2001188.
5. X. Wu, Y. Z. Liu, F. Qi, F. Lin, H. T. Fu, K. Jiang, S. F. Wu, L. Y. Bi, D. Wang, F. Xu, A. K. Y. Jen and Z. L. Zhu, *J. Mater. Chem. A*, 2021, **9**, 19778-19787.
6. K. Lang, Q. Guo, Z. W. He, Y. M. Bai, J. X. Yao, M. Wakeel, M. S. Alhodaly, T. Hayat and Z. A. Tan, *J. Phys. Chem. Lett.*, 2020, **11**, 9596-9604.
7. P. Wang, W. Li, O. J. Sandberg, C. H. Guo, R. Sun, H. Wang, D. H. Li, H. J. Zhang, S. L. Cheng, D. Liu, J. Min, A. Armin and T. Wang, *Nano Lett.*, 2021, **21**, 7845-7854.
8. W. Chen, D. Li, X. Chen, H. Chen, S. Liu, H. Yang, X. Li, Y. Shen, X. Ou, Y. Yang, L. Jiang, Y. Li and Y. Li, *Adv. Funct. Mater.*, 2022, **32**, 2109321.
9. L. Liu, Z. Xiao, C. Zuo and L. Ding, *J Semicond*, 2021, **42**, 020501.
10. X. Gu, X. Lai, Y. Zhang, T. Wang, W. L. Tan, C. R. McNeill, Q. Liu, P. Sonar, F. He, W. Li, C. Shan and A. K. K. Kyaw, *Adv. Sci.*, 2022, **9**, 2200445.
11. H. Yang, W. Chen, Y. Yu, Y. Shen, H. Yang, X. Li, B. Zhang, H. Chen, Q. Cheng, Z. Zhang, W. Qin, J.-D. Chen, J.-X. Tang, Y. Li and Y. Li, *Adv. Mater.*, 2023, **35**, 2208604.
12. S.-Q. Sun, X. Xu, Q. Sun, Q. Yao, Y. Cai, X.-Y. Li, Y.-L. Xu, W. He, M. Zhu, X. Lv, F. R. Lin, A. K. Y. Jen, T. Shi, H.-L. Yip, M.-K. Fung and Y.-M. Xie, *Adv. Energy. Mater.*, 2023, 2204347.